Computational modeling of heat transfer in rotating heat pipes using nanofluids: A numerical study using PSO

Ziya Uddin, Souad Harmand, Shahid Ahmed

International Journal of Thermal Sciences 112 (2017) 44-54

Computational modeling of heat transfer in rotating heat pipes using nanofluids: A numerical study using PSO

Ziya Uddin [a, *], Souad Harmand [b], Shahid Ahmed [a]

[a] SoET, BML Munjal University, Gurgaon, Haryana 123413, India
[b] UVHC, Valenciennes, France

1. Introduction

Rotating machines are devices that convert electrical energy into mechanical energy or conversely, the mechanical energy into electrical energy. In such machines, heat is generated as a result of the electrical and mechanical losses inside the machine which can cause overheating and hence, can reduce the machine performance as well as its lifespan. Therefore managing the thermal dissipation for maintaining temperature in the specified range is crucial for the safety and reliability in numerous engineering domains. A general solution for this problem is to insert a cylindrical heat pipe within the axis of rotation of the rotating machine as well as inside the various gaps between the axis and other parts of the machine to extract its heat and reduce its temperature. In this process, the pipe rotates or revolves at the speed of the machine. Rotating and revolving heat pipes have been successfully studied and used in cooling rotating machinery and generators for decades [1–7].

The thermal performance of the heat pipe depends upon its geometry, structure and the working fluid inside the heat pipe. Therefore, to improve the thermal performance of a heat pipe having fixed geometry compatible with the machine, the working fluid with improved thermal properties has to be used. But common fluids like water, ethylene glycol and oil etc. have low thermal conductivities. On the other hand, metals and their oxide have high thermal conductivities compared to these fluids. A uniform dispersion of low concentration nano-size metal/metal-oxide particles into the base fluid can enhance the thermal conductivity; these fluids containing nano-size particles are called nano-fluids [8]. This concept attracted various researchers towards nano-fluids, and various theoretical and experimental studies have been conducted to find the thermal properties of nano-fluids [9–12]. It has been observed that the thermal conductivity of nano-fluids depends on various factors e.g., particle material, base fluid material, particle volume fraction, particle size, particle shape, temperature, nano-particle Brownian motion, nano-particle-base fluid interfacial layers, and particle clustering etc. [9]. It is also found that the insertion of nano-particle increases the viscosity of the fluid [10]. Chon et al. [11] found an empirical correlation for the thermal conductivity of nano-fluid within the particle size range from 11 nm to 150 nm and temperature range from 21 °C to 71 °C. They reported that, Brownian motion of nano-particles constitutes a key mechanism of the thermal conductivity enhancement with increasing temperature and decreasing nano-particle sizes. But this empirical formula was valid only for water-Al_2O_3 nano-fluid. Very recently, Massimo [12] analyzed the experimental data of thermal conductivity and viscosity of nano-fluids, obtained by various researchers for different types of nano-particles dispersed in different base fluids, and found an empirical correlating equation for the prediction of effective dynamic viscosity and thermal conductivity of nano-fluids.

With the advances in thermal properties and viscosity of nano-fluids, the flow of nano-fluids in various engineering processes has been studied by various authors. Rashidi et al. have studied the nano-boundary-layer flow over stretching surfaces in different conditions such as isothermal permeable sheet with transpiration and in the presence of thermal radiations [13–15]. An experimental study on thermal performance of a disk-shaped miniature heat pipe with nano-fluid showed that the use of nano-fluid reduces the thermal resistance of heat pipes [16]. Shung et al. have experimentally studied the thermal performance of grooved circular heat pipe with silver-water nano-fluid [17]. Yu-Hsing et al. studied the thermal performance of Pulsulating heat pipe in presence of silver nano-fluid [18]. Paisarn et al. have observed the enhancement in performance of cylindrical heat pipe with refrigerant-titanium nano-fluid [19]. Shuangfeng et al. investigated pulsulating heat pipe with functional thermal fluids [20]. Furthermore, the study

* Corresponding author.
E-mail address: ziya_dd@rediffmail.com (Z. Uddin).

DOI : 10.1016/j.ijthermalsci.2016.09.035

shows that alumina-water nano-fluid can enhance the heat transfer performance of cylindrical heat pipe [21]. Karthikeyan et al. studied the effect of nano-fluids on thermal performance of closed loop pulsating heat pipe experimentally and reported that the nano-fluid enhance the heat transfer limit by 33.3% [22]. A detailed description about the use of nano-fluids in different heat pipes can be found in the review article by Zhen-Hua et al. [23].

These studies involving the heat pipes with nano-fluid are experimental and only a few theoretical/numerical studies have been reported [24–27]. To the best of our knowledge, none of these studies involve the rotating heat pipe with nano-fluids. The scope of the present work is to implement the appropriate numerical models for the properties of nano-fluids that satisfy a wide range of experimental data, and study the effects of fluid mass to be inserted in the pipe, rotation speed of the machine, nano-particle size and nano-particle concentration on heat transfer performance of rotating cylindrical heat pipes. To solve the non-linear differential equations governing the flow of nano-fluids inside the heat pipe and the heat transfer equation, a new methodology based on particle swarm optimization (PSO) has been considered.

2. Mathematical formulation

In the present model, it is assumed that the rotation speed of the machine/pipe is high, so that the effect of gravity is negligible compared to the centrifugal force. Liquid inertia is small and the liquid film thickness is very much smaller than the radius of the pipe. Radiation and convection terms are negligible and, no slip conditions have been used at the boundaries. Physical model and co-ordinate system are given in Fig. 1. Figure depicts that heat supplied to the pipe from evaporator section causes vaporization of the liquid and due to pressure difference between condenser and evaporator section, the vapors flow from evaporator section to condenser section through adiabatic zone of the heat pipe (from left to right in the figure). The vapors are condensed into liquid inside the condenser zone and due to high rotation of the pipe, the centrifugal force keeps this liquid in contact with the wall of the pipe which then moves from right to left inside the pipe. The geometry of the pipe is cylindrical, and the liquid film thickness is assumed to be very small as compared to the radius of the pipe. The heat transfer is considered as 1 D conductive heat transfer through the liquid layer perpendicular to the liquid flow direction. Therefore, Cartesian coordinate system has been taken into account, where x-axis is taken along the wall of the pipe.

Taking the control volume in the liquid film and analyzing static force balances in x and y directions result in the following equations:

$$\text{X}-\text{direction momentum}: \rho_{nf}\omega^2 r\sin\alpha - \frac{\partial P_{nf}}{\partial x} + \frac{\partial \tau_{nf}}{\partial y} = \rho_{nf}u_{nf}\frac{\partial u_{nf}}{\partial x} \quad (1)$$

where τ_{nf} is liquid shear stress.

$$\textbf{Y-direction momentum}: -\rho_{nf}\omega^2 r\cos\alpha - \frac{\partial P_{nf}}{\partial y} = \rho_{nf}u_{nf}\frac{\partial u_{nf}}{\partial x} \quad (2)$$

First term in Equations (1) And (2) is due to the centrifugal force on the liquid control volume resulted by the axial rotation of heat pipe.

Following Remi Bertossi et al. [7], the mass flow rate at the extremities of the pipe are taken as zero. Therefore the boundary conditions at the evaporator/condenser end are:

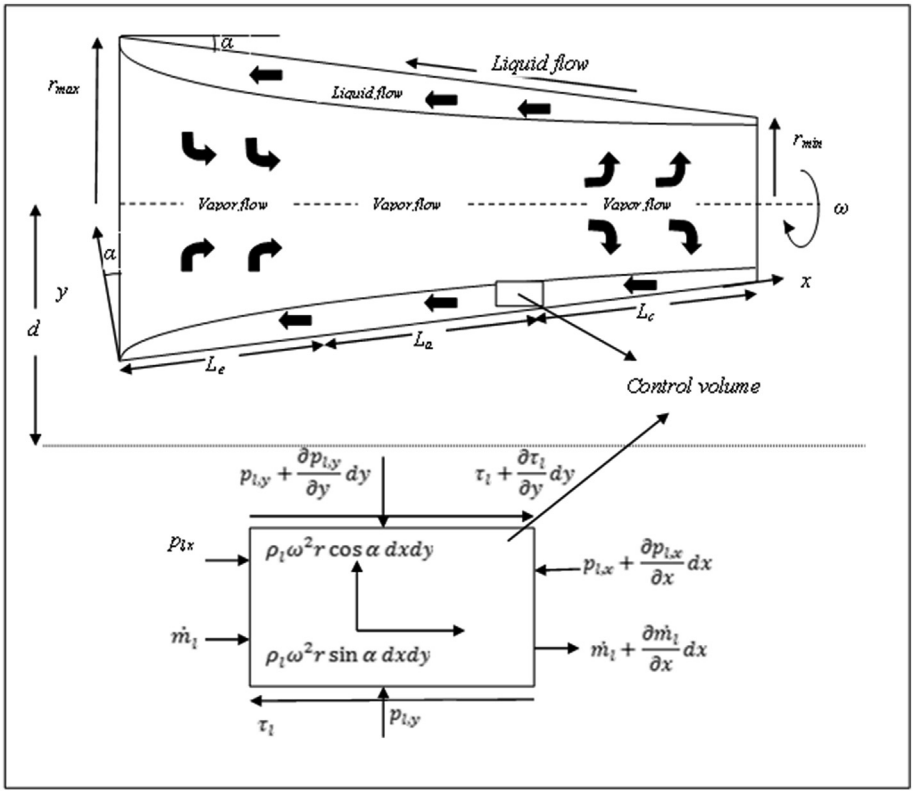

Fig. 1. Physical model and coordinate system.

At evaporator end, $x = 0$ and condenser end $x = L_t \quad \dot{m}_l = 0$ (3)

where L_t is the total length of the pipe and $\dot{m}$ is mass flow rate per unit length.

At the wall of the pipe no slip condition has been assumed, therefore at, $y = 0\ u_{nf} = 0$ (4)

At Liquid/vapor interfaces:

$$y = \delta,\ \tau_{nf,\delta} = \mu_{nf}\frac{\partial u_{nf}}{\partial y} = \frac{d\,\dot{m}_l}{dx}\left(\overline{w}_v \cos\ \alpha + u_{nf,\delta}\right) \tag{5}$$

where δ is the liquid film thickness inside the pipe, $\overline{w}_v$ and $u_{nf,\delta}$ are average vapor velocity in axial direction of the pipe and liquid velocity at the interface. ρ_{nf} is nano-fluid viscosity, ω,r and α are rotational speed, radius and taper angle of the pipe respectively. P_{nf} and τ_{nf} are pressure and shear stress due to nano-fluid at the interface respectively.

The liquid inertia term in eq. (1) and eq. (2) is of second order in magnitude compared to other force terms and can be neglected. Eliminating P_{nf} from eqs. (1) and (2) and using condition at y = 0 and at the interface, we can find the expression for u_{nf} as given below.

$$u_{nf} = \frac{1}{\mu_{nf}}\frac{\partial P_v}{\partial x}\left(\frac{y^2}{2} - \delta y\right) + \frac{\rho_{nf}}{\mu_{nf}}\omega^2 r\left(\sin\alpha - \cos\alpha\frac{\partial\delta}{\partial x}\right)\left(\frac{y^2}{2} - \delta y\right) - \frac{y}{\mu_{nf}}\tau_{v,\delta}\cos\alpha - \frac{y}{\mu_{nf}}\frac{d\,\dot{m}_l}{dx}\left(\overline{w}_v\cos\alpha + u_{nf,\delta}\right) \tag{6}$$

where P_v and $\tau_{v,\delta}$ are pressure and shear stress due to vapor at the interface respectively.

Song et al. [4] proved that for high speed rotating pipes the shear stress at the interface due to vapor and the vapor pressure is very small in comparison to other terms. So these terms can be neglected. Also the velocity $u_{nf,\delta}$ is very small in comparison of the term $\overline{w}_v \cos\alpha$ and hence, it can also be dropped. Using these assumptions eq. (6) takes the following form:

$$u_{nf} = \frac{\rho_{nf}}{\mu_{nf}}\omega^2 r\left(\sin\alpha - \cos\alpha\frac{\partial\delta}{\partial x}\right)\left(\frac{y^2}{2} - \delta y\right) - \frac{y}{\mu_{nf}}\frac{d\,\dot{m}_l}{dx}(\overline{w}_v\cos\alpha) \tag{7}$$

With the help of eq. (4) the expression for mass flow rate ($\dot{m}$) can be found by integrating $\rho_{nf}u_{nf}$ with respect to y within the limits 0 to δ.

Therefore,

$$\dot{m}_l = \frac{\rho_{nf}}{\mu_{nf}}\omega^2 r\left(\sin\alpha - \cos\alpha\frac{\partial\delta}{\partial x}\right)\left(\frac{\delta^3}{3}\right) - \frac{1}{\mu_{nf}}\frac{d\,\dot{m}_l}{dx}(\overline{w}_v\cos\alpha)\frac{\delta^2}{2} \tag{8}$$

2.1. Heat transfer assessment

It is assumed that the liquid film thickness is very much small. Therefore, the heat transfer through the heat pipe is only because of the conduction between thin liquid film layer, wall and the liquid vapor interface. Considering 1 D conductive heat transfer through the liquid layer perpendicular to the liquid flow direction gives the following equation:

$$\frac{d^2T}{dy^2} = 0$$

Integrating this equation implies : $T = C_1 y + C_2$ (9)

At the wall of the pipe: y=0, T=T_w and $-k_{nf}\left(\frac{\partial T}{\partial y}\right)_{y=0} = Q_{e/c}(x)$

At liquid vapor interface: y=δ, T=$T_{sat}$where Tw is the temperature at the wall of the heat pipe, T_{sat} is saturation temperature at liquid vapor interface, $Q_{e/c}(x)$ is thermal flow density in evaporator/condenser and k_{nf} is the thermal conductivity of the nano-fluid.

Using these conditions, the thermal flow density in evaporator/condenser is written as,

$$Q_{e/c}(x) = \frac{k_{nf}(T_w - T_{sat})}{\delta} \tag{10}$$

considering change of phase and assuming that $\overline{h}_{fg}$ is the average enthalpy change of vapor in condensing to a liquid and subcooling to the average liquid temperature of the film and vice versa. Then,

$$Q_{e/c}(x) = -h_{fg}\frac{d\,\dot{m}_l}{dx} \tag{11}$$

Following Daniels et al. [2], we can write $\overline{h}_{fg} = h_{fg} + 0.35C_p(\Delta T)$ Combining eqs. (8) and (9) we get

$$\frac{d\,\dot{m}_l}{dx} = -\frac{k_{nf}(T_w - T_{sat})}{\overline{h}_{fg}\delta} \tag{12}$$

Rearranging the terms in eq. (5) and using (9), we get,

$$\frac{d\delta}{dx} = \tan\alpha + \frac{3k_{nf}(T_w - T_{sat})}{2\overline{h}_{fg}\rho_{nf}\omega^2 r}\frac{\overline{w}_v}{\delta^2} - \frac{3\mu_{nf}}{{\rho_{nf}}^2\omega^2 r\cos\alpha}\frac{\dot{m}_l}{\delta^3} \tag{13}$$

Song et al. [4] proved that for high speed rotating pipes the shear stress at the interface due to vapor and the vapor pressure is very small in comparison to other terms; therefore, only liquid flow modeling is taken into consideration. Here it is assumed that the whole energy entering into the evaporator section converts the liquid into vapor. Therefore, the average vapor velocity can be obtained by the relation $Q_e = \rho_v \overline{w}_v h_{fg}$

$$\Rightarrow \overline{w}_v = \frac{k_{nf}(T_w - T_{sat})}{\delta\rho_v h_{fg}} \tag{14}$$

In this formulation r depends on the taper angle and given by the formula: r=R_{max}−$x\sin\alpha$

2.2. Nano-fluid properties

$$\rho_{nf} = \phi\rho_p + (1-\phi)\rho_f \tag{15}$$

$$(\rho C_p)_{nf} = \phi(\rho C_p)_p + (1-\phi)(\rho C_p)_f \tag{16}$$

where ϕ is nano-particle concentration in pure fluid, ρ_p and ρ_f are the density of nano-particle and the pure fluid respectively. $(C_p)_p$ and $(C_p)_f$ are the specific heat of nano-particle and pure fluid respectively.

Following Massimo [12] the viscosity of nano fluid is given by:

$$\mu_{nf} = \frac{\mu_f}{1 - 34.87\left(d_p / d_f\right)^{-0.3} \phi^{1.03}} \tag{17}$$

$$d_f = 0.1\left[\frac{6M}{N\pi\rho_{fo}}\right]^{1/3}$$

where d_f is the diameter of base fluid molecule, M is the molecular weight of the base fluid, N is the Avogadro number, and ρ_{fo} is the mass density of the base fluid calculated at the reference temperature (293 K).

Since the nano-particles are not considered in vapor phase, therefore the phase change enthalpy (h_{fg}) of the nano-fluid will be due to the pure fluid only and specified by the following relation:

$$\left(\rho h_{fg}\right)_{nf} = (1 - \phi)\left(\rho h_{fg}\right)_f \tag{18}$$

Following Shafahi et al. [25], the thermal conductivity of nano fluid is given by:

$$k_{nf} = \left[\frac{k_{pe} + 2k_b + 2(k_{pe} - k_b)(1 - \beta)^3\phi}{k_{pe} + 2k_b + 2(k_{pe} - k_b)(1 - \beta)^3\phi}\right] k_b \tag{19}$$

$$k_{pe} = \gamma\left[\frac{2(1 - \gamma) + (1 - \beta)^3(1 + 2\gamma)}{-(1 - \gamma) + (1 - \beta)^3(1 + 2\gamma)}\right] k_b \tag{20}$$

$$\gamma = \frac{k_{layer}}{k_p}$$

$$\beta = \frac{h}{r_p}$$

Here k_{layer} is the thermal conductivity of the nano layer formed by the base fluid particles around nano particle in the nanofluid, and h is the thickness of this thermal layer. Following Yu et al. [8], $k_{layer} = 100k_f$ and $h = 2$ nm have been considered during computations.

Table 2
Thermal properties of CuO and EG at reference temperature (293 K).

	CuO	EG
ρ	6500	1105.2
C_p	540	2452.9
K	18	0.2546
μ	–	0.0118
h_{lv}		800000
M		0.06207
ρ_{fo}		1112.1
ρ_v		9.2

In the heat transfer analysis, the heat flux (Q) is calculated by using the formula $Q = \dot{m}_l h_{lv}.2\pi r$, where $\dot{m}_l$ is the lineic mass flow rate of the fluid inside the pipe. Therefore, Q is expressed in units of watts (W).

3. Method of solution

3.1. Particle swarm optimization (PSO)

Particle swarm optimization (PSO) (Riccardo et al. [28]) is one of the evolutionary algorithms that simulate the behavior of bird flocking and fish schooling etc. When a flock of birds search for food, the birds find food through social cooperation with other birds in the neighborhood. Initially all birds move randomly, but after a while all the birds follow the bird who is nearest to the food. Particle swarm optimization utilizes a population of particles that fly through the problem hyperspace with given velocities. In each iteration, the velocity of individual particle is stochastically adjusted according to its historical and neighborhood best positions. The particle best and the neighborhood best are derived according to a user defined fitness function. The movement of each particle naturally evolves to an optimal or near optimal solution. Every particle remembers its own previous best value as well as the neighborhood best. All particles are then informed about the most successful particle to improve them.

In PSO, the term particle refers to a population member who is massless and volume-less that is subject to velocity and acceleration towards a better mode of behavior. Each particle keeps track of

Table 1
Comparision of the results with previously published work.

Parameters	Notation	Value
Fluid used	–	water
Saturation temperature (°C)	T_{sat}	100
Rotation speed (rpm)	ω	3000
Wall temperature at the evaporator (°C)	T_{evap}	120
Mass of the fluid introduced in the pipe (kg)	M	0.001
Liquid density (kg m^{-3})	ρ_l	958.34
Vapor density (kg m^{-3})	ρ_v	0.59837
Change of phase enthalpy (J kg^{-1})	h_{lv}	2256390
Liquid thermal conductivity (W m^{-1} K^{-1})	λ_l	0.6791
Liquid viscosity (Pa s)	μ_l	0.000283
Vapor viscosity (Pa s)	μ_v	1.23×10^{-5}
Radius of the heat pipe (m)	R	4×10^{-3}
Evaporator length (m)	L_e	0.04
Condenser length (m)	L_c	0.042
Total length of the heat pipe (m)	L_T	0.2

Results of the calculation	Remi Bertossi et al. [7]	Present
Average value of the liquid film thickness along the heat pipe (m)	2.1×10^{-4}	$2.110178659396615 \times 10^{-4}$
Liquid film thickness at the evaporator (m)	1.88×10^{-4}	$1.82691452163402 \times 10^{-4}$
Liquid film thickness at condenser (m)	2.33×10^{-4}	$2.30241531518841 \times 10^{-4}$
Total flux exchanged in the heat pipe (W)	73	72.886594875732442

Table 3
Thermal conductivity and viscosity of CuO+EG nano fluid.

	d_p	5	10	15	20	25	30
$\phi = 0.04$	k_{nf}	0.3292	0.2896	0.2847	0.2836	0.2833	0.2833
	μ_{nf}	0.0176	0.0161	0.0155	0.0151	0.0148	0.0146
	ϕ	0	0.01	0.02	0.03	0.04	0.05
$d_p = 10$ nm	μ_{nf}	0.0118	0.0126	0.0136	0.0148	0.0161	0.0178
	k_{nf}	0.2546	0.2626	0.2711	0.2801	0.2896	0.2997
	ρ_{nf}	1105.2	1159.1	1213.1	1267.0	1321.0	1374.9
	Cp_{nf}	2452.9	2345.6	2247.9	2158.5	2076.4	2000.7

its coordinates in the problem space which are associated with the best solution (objective function to be optimized) achieved so far. This value is called '*pbest*'. The particle also keeps track of the best value obtained so far by any particle in the neighborhood. This value is called '*lbest*'. The particle swarm optimization consists of at each time step, changing the velocity of each particle towards its '*pbest*' and '*lbest*'. In PSO a fitness function is defined which is to be optimized (minimize for the present case). Initially a number of random solutions of the problem are generated in the search space. At each iteration the value of fitness function are calculated for each particle and two minimum values of the fitness function are found.

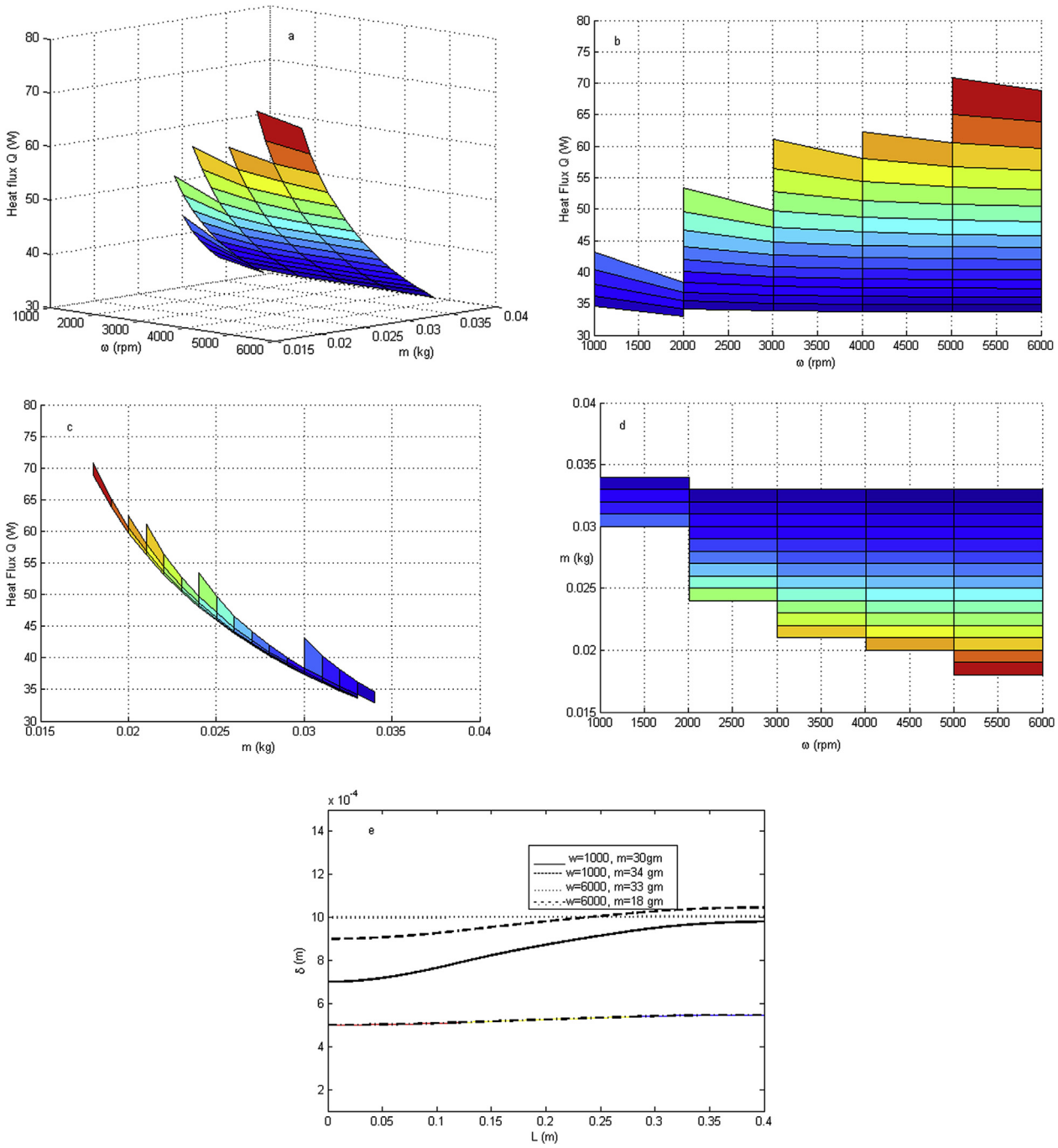

Fig. 2. Dependence of heat transfer on input nano fluid mass and rotation speed of the pipe.

The first value is named as 'pbest' and the second value is called 'Ibest'. Each particle's velocity and position are updated by the following equations.

$$v[\,] = \psi * v[\,] + \phi_P * rand() * (pbest[\,] - x[\,]) + \phi_g * rand() * (Ibest[\,] - x[\,]) \quad (21)$$

$$x[\,] = x[\,] + v[\,] \quad (22)$$

Here, $x[\,]$ and $v[\,]$ are the particle position and velocity respectively. *rand( )* is a random number in the range [0,1]. ϕ_p ϕ_g and ψ are the positive parameters of PSO known as local weights and inertial weigh respectively. Large values of ψ facilitates the global search while its small value facilitates the local search. To control the maximum velocities of the particles and for efficient working of PSO to search the global optima we took $\phi_p = \phi_g = 1.49618$ and $\psi = 0.7298$(See Riccardo et al. [28]).

3.2. Implementation of PSO

The ordinary differential Equations (12) and (13) are first-order coupled simultaneous equations. To solve this system we require two initial conditions but we have only one initial condition that is the liquid mass flow rate $\dot{m}_l$ which is zero at the ends ($x = 0$ and $x = L_T$) of the pipe. The initial condition for liquid film thickness δ is not known. Amongst the three sections in the heat pipe, namely evaporator, adiabatic zone and condenser, only the temperature of the evaporator is known and is equal to the temperature of the machine whose temperature is to be reduced. The temperature of the adiabatic zone is considered to be equal to the temperature of adjacent surrounding of the hot machine. The temperature of the condenser section is not known, which has to be evaluated to compute the heat transferred. Therefore, in order to solve the non-linear differential Equations (12) and (13), we have to first find the liquid film thickness δ at the evaporator end and the temperature of the condenser section T_{cond}. These values for δ and T_{cond} are found by using the PSO algorithm described above. First of all, a random population of solution for the problem is found by solving Equations (12) and (13) for random values of δ and T_{cond} by using Runge Kutta Fehlberg integration scheme and hence, the liquid film profile inside the pipe. After getting the liquid film profile inside the heat pipe, the average total mass of the fluid inside the pipe and total heat transferred in each section of the pipe are calculated. To achieve the optimization of film thickness at the evaporator end and the condenser temperature, the objective function (fitness function for PSO) to be minimized is: $Min = (Q_{cond\_end}/Q_{adia})^2 + ((avg_{totmass} - m_0)/avg_{totmass})^2$.

Here Q_{cond_end} is heat flux at $x = L_T$, Q_{adia} is the heat flux along adiabatic zone, m_0 is the mass of the fluid inserted in the pipe initially and $avg_{totmass}$ is the average mass calculated through the present model. For significant results, the following conditions are also applied along with the above fitness function.

Film thickness at the end of evaporator $(\delta_0) >= 0$.

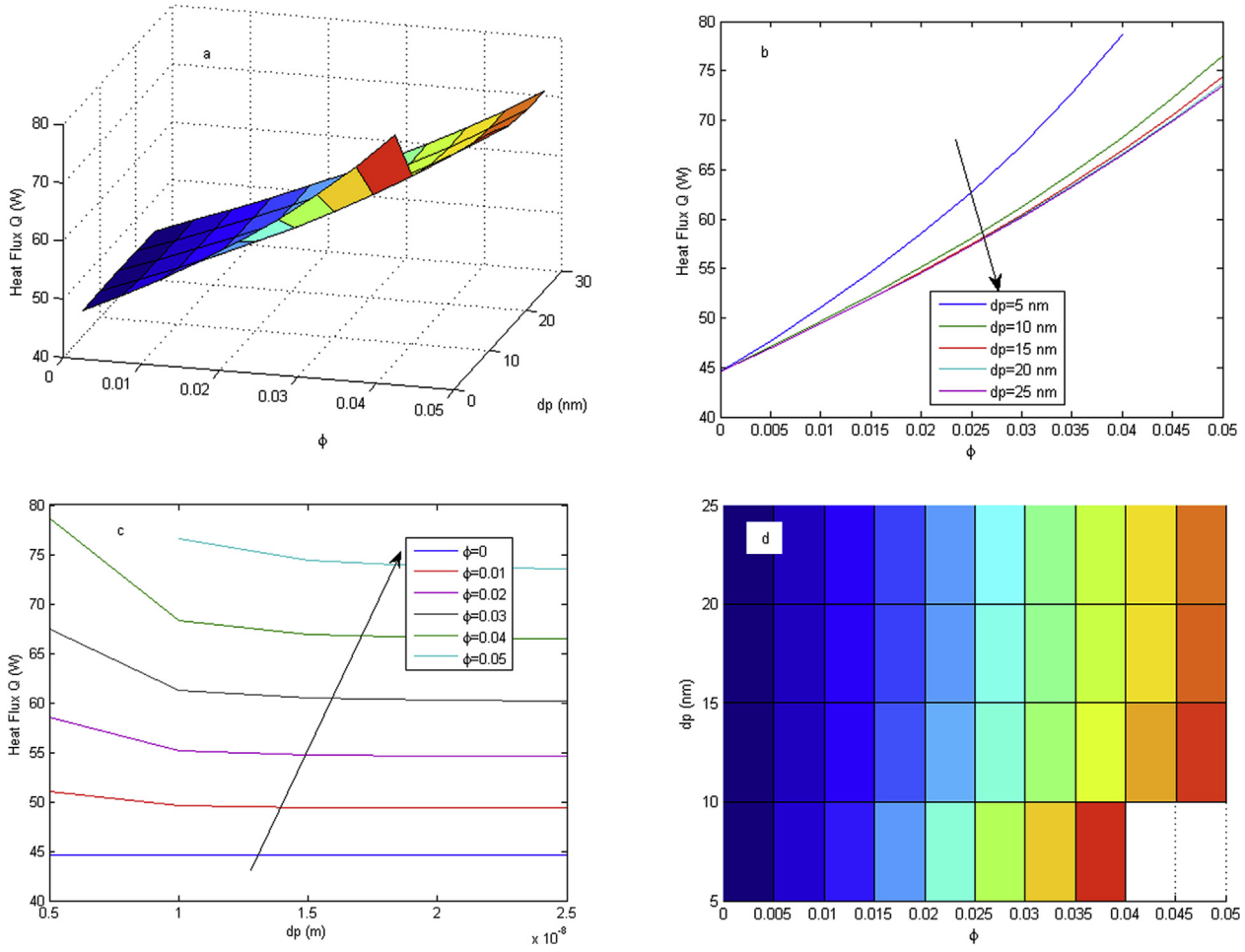

Fig. 3. Dependence of heat transfer on nanoparticle concentration and nano paticle size.

Heat entered in the pipe through evaporator ≅ Heat taken out via condenser.

In PSO algorithm, an optimized solution is usually achieved in a number of iterations using a random approach. Therefore, to get the solution of the problem by using the methodology discussed above, we ran a MATLAB code until it satisfied the condition Min≤ 10^{-08}. For each iteration, the random population size is taken as 200.

4. Results and discussion

To validate the mathematical formulation and the MATLAB code, a comparison of the results obtained has been done with previously published work, taking pure water (without nano-particles) as working fluid. The comparison of the results is given in the following Table 1.

In the present work the computations have been carried out for the CuO+EG (ethylene glycol) nano-fluid under different conditions. The thermo-physical properties of pure CuO and pure EG at reference temperature and the thermo-physical properties of the CuO+EG nano-fluid are given in Tables 2 and 3 respectively.

The effects of various parameters involved in the problem on the heat transfer through the heat pipe have been calculated and the conditions for the maximum heat transfer have been found. The evaporator temperature of the pipe has been considered equal to the temperature of the rotating machine whose heat is to be removed with the help of the pipe. The temperature at the interface of the liquid and vapor phase inside the heat pipe has been considered equal to the temperature of the adiabatic zone of the heat pipe. The calculations have been done for cylindrical pipe (α=0) of radius 1 cm the lengths of condenser, adiabatic and evaporator sections of the pipe are 12 cm, 16 cm and 12 cm respectively. Temperature of evaporator zone and saturation temperature have been assumed to be 130 °C and 100 °C respectively. Whole computational analysis can be divided in the following sections.

4.1. Dependence of heat transfer on input nano-fluid mass and rotation speed of the pipe

In the numerical calculations the nano particle concentration and nanoparticle diameter have been taken as 0.05 and 10 nm respectively. The effect of working fluid (nano fluid) mass inserted inside the pipe and the rotation speed of the pipe on heat transfer is shown as 3D plot in Fig. 2a. From this figure it is clear that the heat transfer decreases with the increase in nano fluid mass inserted inside the pipe, but it increases with the increase in rotational speed of the pipe. Fig. 2b–d are the 2D view of Fig. 2a. Fig. 2b depicts that the heat transfer is maximum for the rotation speed between 5000 and 6000 rpm. For the heat pipe, there is a particular value of working fluid mass for which the heat transfer is maximum. Below this mass there will be a condition of dry out in the pipe and above this mass there will be fluid accumulation inside the condenser section of the heat pipe. Therefore, for the

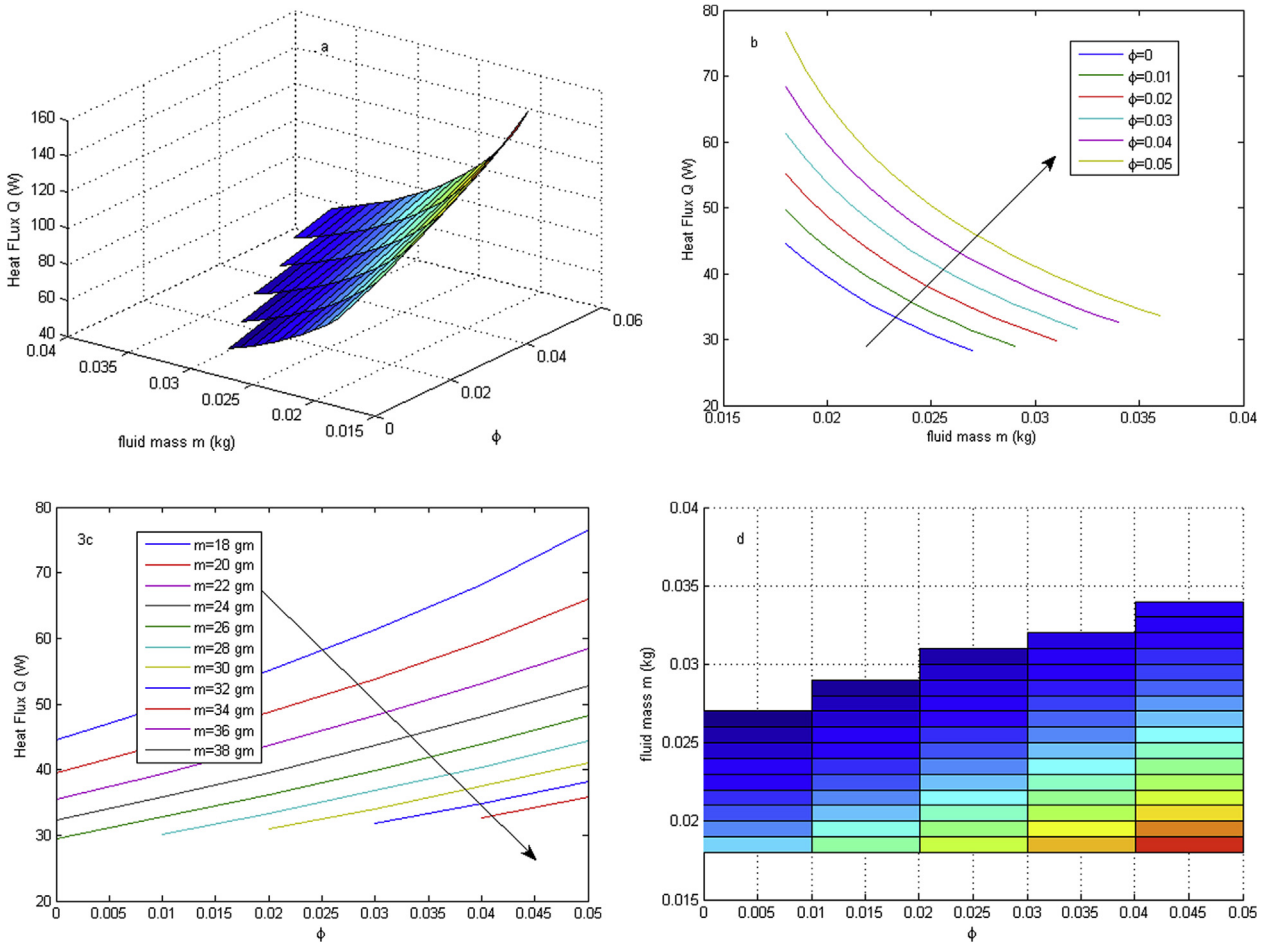

Fig. 4. Dependence of Heat transfer on input mass and nano particle concentration.

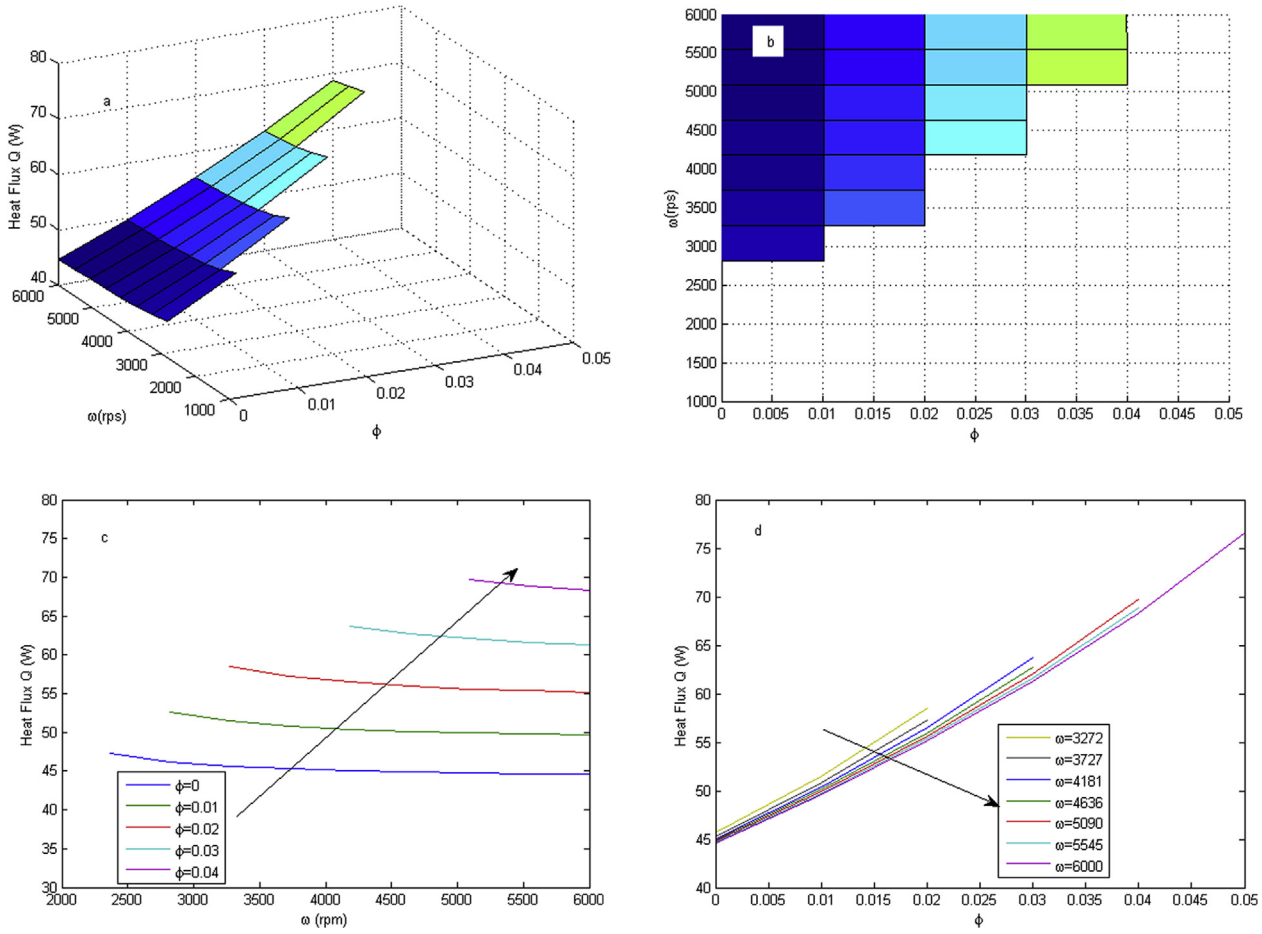

Fig. 5. Dependence of Heat transfer on rotation speed and nano particle concentration.

efficient working of the heat pipe there is a particular fluid mass range. From Fig. 2d, it is observed that for the rotation speed 1000–2000 rpm the working fluid mass range is 30–34 gm. This means that if we introduce the fluid beyond this range, there will be either the dry or there will be fluid accumulation inside the pipe. As the speed of the pipe increases beyond 2000 rpm the upper limit for the fluid mass is almost 33 g for all the rotation speeds upto 6000 rpm, but the lower limit of the fluid mass decreases. For the rotation speed 5000–6000 rpm, the working nano-fluid mass range is 18–33 gm. From Fig. 2c it is clear that the maximum heat transfer is for the 18 g of nano-fluid inside the pipe. The heat transfer through the heat pipe depends upon the liquid film thickness inside the heat pipe; thinner the liquid film, higher will be the heat transfer. Fig. 2e depicts that for the rotation speed of 6000 rpm with nano-fluid mass of 18 g, liquid film is thinnest; therefore, the heat transfer is maximum for this case. The dependence of mass range on the rotation speed of the pipe is due to the fact that the rotation of the pipe drags the fluid from the condenser section of the pipe to the evaporator section through the adiabatic zone. As the rotation speed of the pipe increases, the centrifugal force on the fluid increases. Hence, more fluid can be transferred from the condenser to evaporator.

4.2. Dependence of heat transfer on nano-particle concentration and nano-paticle size

In this section, the computations have been done for 18 g of CuO+EG nano fluid in the rotating pipe with rotation speed of 6000 rpm. The 3D representation of heat transfer on nano particle concentration and nano particle diameter is shown in Fig. 3a. Fig. 3b–d are 2D view of Fig. 3a. Fig. 3b and c depict that heat transfer decreases with the increase in particle size, but it increases with the increase in nanoparticle concentration. The maximum possible concentration for the 5 nm size particle is 0.04 and this is the optimal concentration for the maximum heat transfer at the considered rotation speed and nano fluid mass. From Fig. 3c, it is also clear that if the nano particle size is more than 10 nm, heat transfer will increase with further increase in nano particle concentration beyond 0.04. The reason for this behavior can be explained with the help of Table 2. From Table 2, it is clear that with the increase in nano particle diameter the thermal conductivity of the nano fluid decreases for a fixed value of nano particle concentration. This results in the decrease in heat transfer rate. The increase in nano particle concentration for fixed size of nanoparticles thermal conductivity also increases whereas the viscosity decreases. Decrease in viscosity helps in the fast movement of nanofluid from condenser to evaporator section and the increased thermal conductivity enhances the heat transfer rate. The variation in thermal conductivity and viscosity of nano fluid with nano particle size and nano particle concentration can also be confirmed with the experimental results of Xiang et al. [10]. In Fig. 3d, the blank portion shows that for the effective working of heat pipe in the presence of nano particles of size 5–10 nm, the maximum possible concentration of nano particle is 0.04.

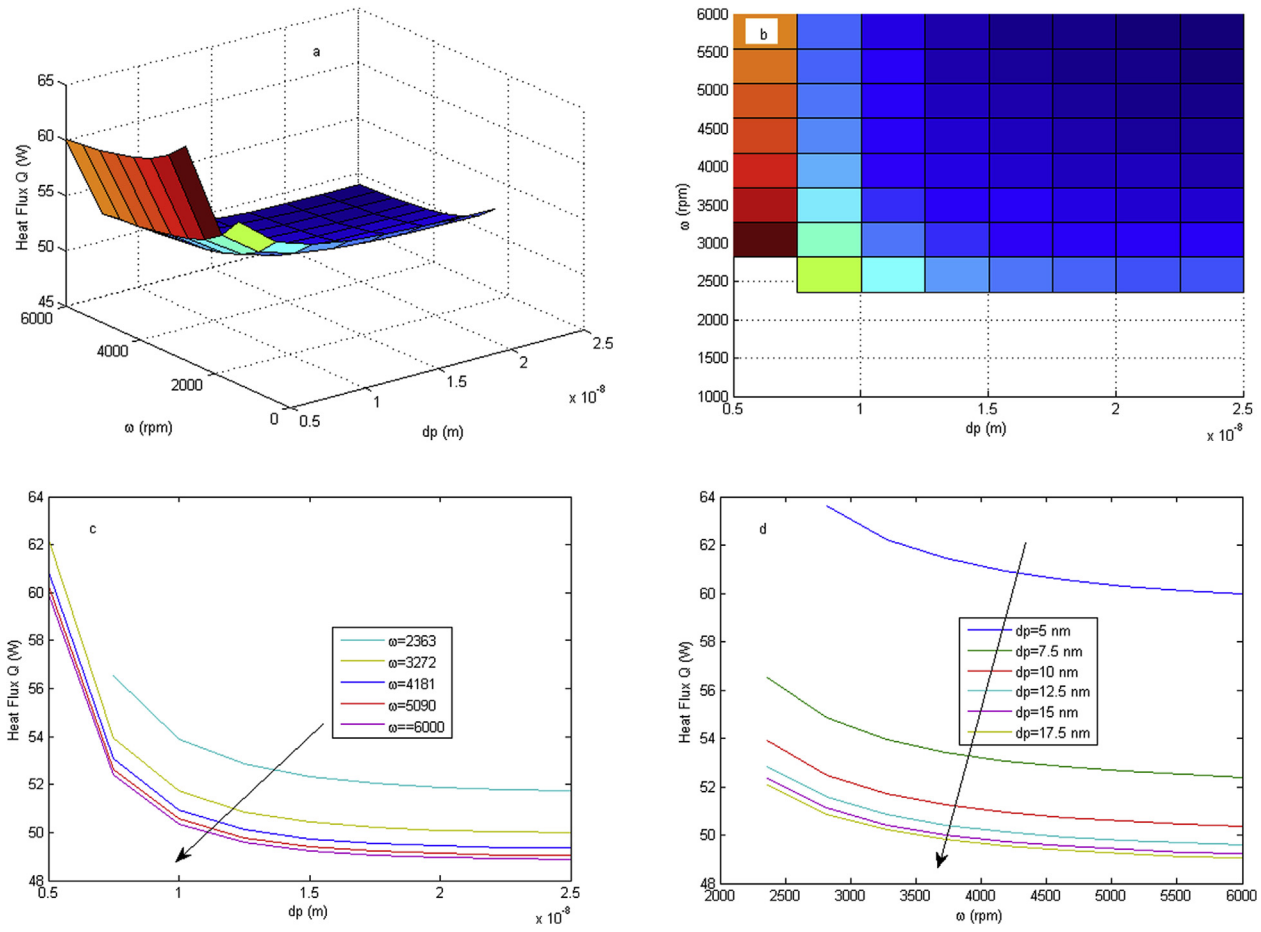

Fig. 6. Dependence of Heat transfer on rotation speed and nano particle concentration.

4.3. Dependence of Heat transfer on input mass and nano particle concentration

In this section, the computations have been done for the particle size of 10 nm at rotation speed of 6000 rpm. The upper and lower limits for the nano fluid mass inserted inside the heat pipe with respect to nano particle concentration and heat transferred by the pipe have been found and shown in Fig. 4a. From Fig. 4a, it is clear that the heat transfer is maximum for low value of fluid mass and higher nano particle concentration. Fig. 4b depicts that for a particular value of fluid mass the heat transfer increases with the increase in nano particle concentration. From this figure, it is also observed that the length of curves increases with the increase in nano particle concentration. This means that the range of fluid mass to be inserted inside the heat pipe increases with the increase in nano particle concentration. Fig. 4c shows the variation in heat transfer rate with nano particle concentration for different values of input masses. For a fixed value of input mass the heat transfer increases with the increase in nano particle concentration. With the increase in input mass the heat transfer decreases and also for the proper working of heat pipe the range of nano particle concentration diminishes. e.g., for input mass of 18 g the range is 0−0.05 and for 34 g this range is only 0.04−0.05. Fig. 4d gives the exact range for fluid mass at different concentration levels. e.g. for the concentration from 0 to 0.01, the fluid mass range is 18−27 gm, whereas for concentration of 0.05, the fluid mass range is 18−34 gm. From this section, it is concluded that for smaller values of fluid mass higher concentration of nano particle gives the higher heat transfer rate.

4.4. Dependence of Heat transfer on rotation speed and nano particle concentration

The computations have been done for 18 g of input nano-fluid mass with nano particle size of 10 nm. The numerical results have been plotted and shown in Fig. 5. Fig. 5b−d exhibits the 2D view of Fig. 5a. Fig. 5b shows the admissible range of nano particle concentration for different rotation speeds. It is clear from the figure that for 18 g of nano fluid mass, the admissible range of nano particle concentration is highest i.e. 0−0.04, whereas for the low rotation speed, i.e. around 3000 rpm, admissible range is only 0−0.01. Fig. 5b also depicts that as the rotation speed increases the admissible range for the nano particle concentration also increases. From Fig. 5a, it can be concluded that for high rotation speed and for high nano particle concentration, heat transfer rate is highest. This is because of the fact that, increase in nano particle concentration increases the thermal conductivity of the nano fluid and, high rotation speed of the heat pipe helps in faster movement of the fluid from condenser to evaporator section of the pipe and results in high heat transfer rate. Fig. 5c shows that for a particular value of nano particle concentration, the heat transfer rate decreases slightly with the increase in rotation speed. From Fig. 5d it is observed that, as the nano particle concentration increases the heat transfer rate increases for higher values of rotation speeds.

4.5. Dependence of Heat transfer on rotation speed and nano-particle concentration

The computations done for 25 g of nano fluid with nano particle concentration of 0.05 as shown in Fig. 6a, depicts that smaller size nano particles at high rotation speed of the pipe gives higher heat transfer rates. Dark (colored) portion in Fig. 6b shows the range of nano particle size at different rotation speeds of the heat pipe. In Fig. 6b, at low rotation speed and small nano particle size there is some white portion. This means that at low rotation speed very small size nano particles cannot help in the heat transfer. As the rotation speed increases the admissible range of nano particle size also increases. From Fig. 6c, it is clear that as the nano particle size increases the heat transfer rate decreases very rapidly till 15 nm, but on further increase in the nano particle size, there is a slight decrease in heat transfer rate. Fig. 6d shows the variation of heat transfer with the rotation speed of heat pipe for different values of nano particle diameter. From the figure it can be concluded that with the increase in rotation speed upto 4000 rpm the heat transfer rate decreases rapidly, but on further increase in rotation speed there is negligible change in heat transfer.

5. Conclusions

Heat transfer through the rotating heat pipe containing nano-fluids was studied numerically. It was found that, the heat transfer through the heat pipe depends on various factors. viz., the input nano-fluid mass, rotation speed of the heat pipe, nano-particle size and nano-particle concentration etc. From the present study, it can be concluded that:

For maximum heat transfer there is a particular value of working fluid mass (nano-fluid mass).

For fixed values of nano-particle size and nano-particle concentration, heat transfer is maximum for lower mass of nano-fluid and high rotation speed of heat pipe.

For fixed value of nano-fluid mass and rotation speed, the heat transfer is maximum for high concentration of small sized nano-particles in the base fluid.

For fixed values of nano-particle size and fixed rotation speed of heat pipe, heat transfer is maximum for lower mass of nano-fluid containing high concentration on nano-particles.

For fixed values of nano-fluid mass containing a particular size of nano-particles, the heat transfer is maximum for high rotation speed of the pipe and higher value of nano-particle concentration.

For fixed value of nano-fluid mass containing a particular concentration of nano-particles, the heat transfer is maximum for high rotation speeds of the heat pipe containing nano-fluid with small sized nano-particles.

References

[1] Gray VH. The rotating heat pipe-a wickless Hollow Shaft for Transferring High Heat fluxes. 1969. ASME Paper No. 69-HT-19.
[2] Daniels TC, Al-Jumaily FK. Investigations of the factors affecting the performance of a rotating heat pipe. Int J Heat Mass Transf 1975;18:961–73.
[3] Harley, Faghri A. Two dimensional rotating heat pipe analysis. Tran ASME 1995;117:202–8.
[4] Song F, Ewing D, Ching CY. Fluid flow and heat transfer model for high speed rotating heat pipes. Int J Heat Mass Transf 2003;46:4393–401.
[5] Faghri A. Heat pipe science and technology. Taylor & Francis; 1994.
[6] Song F, Ewing D, Ching CY. Experimental investigation on the heat transfer characteristics of axial rotating heat pipes. Int J Heat Mass Transf 2004;47:4721–31.
[7] Bertossi Remi, Guilhem Noelie, Ayel Vincent, Romestant Cyril, Bertin Yves. Modelling of heat and mass transfer in the liquid film of a rotating heat pipe. Int J Therm Sci 2012;52:40–9.
[8] Yu W, Choi SUS. The role of interfacial layers in the enhanced thermal conductivity of nanofluids: a renovated Maxwell model. J Nanoparticle Res 2003;5:167–71.
[9] Wang Xiang-Qi, Mujumdar Arun S. A review on nanofluids – part I: theoretical and numerical Investigations. Braz J Chem Eng 2008;25(4):613–30.
[10] Wang Xiang-Qi, Mujumdar Arun S. A review on nanofluids – part II: experiments and applications. Braz J Chem Eng 2008;25(4):631–48.
[11] Chon Chan Hee, Kihm Kenneth D, Lee Shin Pyo, Choi SUS. Empirical correlation finding the role of temperature and particle size for nanofluid (Al_2O_3) thermal conductivity enhancement. Appl Phys Lett 2009;87(15). http://dx.doi.org/10.1063/1.2093936. 153107-153107-3.
[12] Corcione Massimo. Empirical correlating equations for predicting the effective thermal conductivity and dynamic viscosity of nanofluids. Energy Convers manage 2011;52:789–93.
[13] Rashidi MM, Erfani E. The modified differential transform method for investigating nano boundary-layers over stretching surfaces. Int J Numer Methods Heat Fluid Flow 2011;21(7):864–83.
[14] Rashidi MM, Freidoonimehr N, Hosseini A, Anwar Beg O, Hung T-K. Homotopy simulation of nanofluid dynamics from a non-linearly stretching isothermal permeable sheet with transpiration. Meccanica 2014;49(2):469–82.
[15] Rashidi MM, Vishnu Ganesh N, Abdul Hakeem AK, Ganga B. Buoyancy effect on MHD flow of nanofluid over a stretching sheet in the presence of thermal radiation. J Mol Liq 2014;198:234–8.
[16] Chien HT, Tsai CY, Chen PH, Chen PY. Improvement on thermal performance of a disk-shaped miniature heat pipe with nanofluid. In: Proceedings of the Fifth International Conference on Electronic Packaging Technology, IEEE, Shanghai, China; 2003. p. 389–91.
[17] Kang Shung-Wen, Wei Wei-Chiang, Tsai Sheng-Hong, Yang Shih-Yu. Experimental investigation of silver nanofluid on heat pipe thermal performance. Appl Therm Eng 2006;26:2377–82.
[18] Lin Yu-Hsing, Kang Shung-Wen, Chen Hui-Lun. Effect of silver nano fluid on pulsulating heat pipe thermal performance. Appl Therm Eng August 2008;28(11–12):1312–7.
[19] Naphon Paisarn, Thongkum Dithapong, Assadamongkol Pichai. Heat pipe efficiency enhancement with refrigerant–nanoparticles mixtures. Energy Convers Manag 2009;50(3):772–6.
[20] Wang Shuangfeng, Lin Zirong. Experimental study on pulsating heat pipe with functional thermal fluids. Int J Heat Mass Transf 2009;52(2009):5276–9.
[21] Yi-Hsuan Hung, Tun-Ping Teng, Bo-Gu Lin. Evaluation of the thermal performance of a heat pipe using alumina nanofluid. Exp Therm Fluid Sci 2013;44:504–11.
[22] Karthikeyan VK, Ramachandran K, Pillai BC, Brusly Solomon A. Effect of nanofluids on thermal performance of closed loop pulsating heat pipe. Exp Therm Fluid Sci April 2014;54:171–8.
[23] Zhen-Hua Liu, Yuan-Yang Li. A new frontier of nanofluid research – application of nanofluids in heat pipes. Int J Heat Mass Transf 2012;55(23–24):6786–97.
[24] Shafahi M, Bianco V, Vafai K, Manca O. Thermal performance of flat-shaped heat pipes using nanofluids. Int J Heat Mass Transf 2010;53:1438–45.
[25] Shafahi M, Bianco V, Vafai K, Manca O. An investigation of the thermal performance of cylindrical heat pipes using nanofluids. Int J Heat Mass Transf 2010;53:376–83.
[26] Do KH, Jang SP. Effect of nanofluids on the thermal performance of a flat micro heat pipe with a rectangular grooved wick. Int J Heat Mass Transf 2010;53:2183–92.
[27] Alizad Karim, Vafai Kambiz, Shafahi Maryam. Thermal performance and operational attributes of the startup characteristics of flat-shaped heat pipes using nanofluids. Int J Heat Mass Transf 2012;55:140–55.
[28] Poli Riccardo, Kennedy James, Blackwell Tim. Particle swarm optimization: an overview. Swarm Intell 2007;1(1):33–57.

Nomenclature

T: Temperature (°C)
m_l: Mass of fluid inserted in the pipe (kg)
L: Length (m)
Q: Heat (Watt)
h_{lv}: change of phase enthalpy (J kg^{-1})
k: thermal conductivity (W m^{-1} K^{-1})
r: radius of heat pipe (m)
P: pressure (Pa)
u: velocity (m s^{-1})
d: diameter (m)
M: Molecular mass of pure fluid (kg)
C_P: specific heat (J $kg^{-1}K^{-1}$)
g: Gravitational acceleration (9.81) (m s^{-2})
N: Avogadro's number ($6.0223 \times 10^{+023}$)
x,y: coordinate axes

Greek symbols

ω: Rotational speed (rpm)
ρ: density (kg m^{-3})
δ: liquid film thickness (m)
μ: viscosity (Pa s)
α: Angle (degree)

τ: Liquid inertia
ϕ: nano particle concentration
β: ratio of nanolayer thickness to nano particle radius
γ: ratio of nanolayer thermal conductivity to nano particle thermal conductivity

Subscripts

w: wall
f: pure fluid (liquid)
nf: nano fluid
p: nano particle
evap: evaporator zone of heat pipe
cond: condenser zone of heat pipe
adia: adaibatic zone of heat pipe
sat: saturation